ARTICLES

Intrinsic Enhancement Factors of the Spin−Orbit Coupling Mechanism Polarization in the Duroquinone−*N*,*N*-Dimethylaniline Derivative Systems

Shinya Sasaki, Yasuhiro Kobori, Kimio Akiyama, and Shozo Tero-Kubota*

Institute for Chemical Reaction Science, Tohoku University, Sendai 980-8577, Japan

Received: May 1, 1998; In Final Form: July 13, 1998

Dynamics of the electron spin polarization of the quinone anion radical generated from the photoinduced electron transfer between duroquinone (DQ) and *N*,*N*-dimethylaniline (DMA) as well as its *p*-halogen substituents (4XDMA) has been investigated by using transient absorption and FTEPR spectroscopies. The radical yield decreased with increasing atomic number of the halogen in the donor. The intrinsic enhancement factors of net absorptive polarization due to the spin−orbit coupling mechanism (SOCM) of $V_{SOCM} = 2$, 17, and 25 were determined in the unit of thermal equilibrium polarization at room temperature for the DQ-4ClDMA, DQ-4BrDMA, and DQ-4IDMA systems, respectively. The net absorptive spin polarization observed has been discussed in terms of SOC interaction of the triplet contact radical ion pair (CRIP) state with the ground state, which is coupled with the singlet CRIP states in the solvent coordinate.

Introduction

Chemically induced dynamic electron polarization (CIDEP) mechanisms have been a subject of study for a long time, because the electron spin polarization created in the initial photochemical process provides fruitful information about the reaction mechanism. The fundamental CIDEP mechanisms, that is, a radical pair mechanism (RPM)[1,2] and a triplet mechanism (TM),[3−5] have been extensively investigated and their mechanisms are well established. Recently, several new mechanisms such as a spin-correlated radical pair mechanism (SCRP),[6,7] a radical-triplet pair mechanism (RTPM),[8−16] and a spin−orbit coupling mechanism (SOCM)[17−24] have been proposed.

The intrinsic enhancement factors of these CIDEP mechanisms are of interest in connection of molecular interactions between open shell molecules. The SCRP mechanism is well-known to give a very large enhancement factor. The quantitative study on the RTPM has produced valuable data concerning the quenching mechanism of excited molecules by paramagnetic species. On the other hand, little is known about the intrinsic enhancement factor on the SOCM. It has been reported that the apparent enhancement factor of the net absorptive polarization increases with increasing atomic number of the heavy atoms in the sensitizers or unexcited electron donors.[21,23] The SOCM is attributed to result from the sublevel selective back electron transfer by SOC interaction. There have been only a few reports on the sublevel selective reactions. Unequal reaction rates for the triplet sublevels were shown for the photochemical decomposition of pyrimidine[25] and tetrazine derivatives[26] at low temperatures. Recent studies of magnetic field effects on the radical yield using transient absorption spectroscopy clarified the influence of the SOC interaction on photoinduced electron transfer reactions in fluid solutions.[17−20] Quantitative investigations on the magnitude of the spin polarization due to SOCM may give important information not only about the interactions between the radicals but also the dissociation process of the contact radical ion pair (CRIP) or exciplex in solutions.

In the present work, heavy atom effects on the radical yield and electron spin polarization were studied for the photoinduced electron transfer reactions between duroquinone (DQ) and *N*,*N*-dimethylaniline (DMA) as well as its halogen derivatives. A quantitative description was given for the analysis of the time profiles of the electron spin polarization in terms of the relevant kinetic and magnetization equations for the quinone anion radicals. The intrinsic enhancement factor of the electron spin polarization and kinetic parameters were determined.

Experimental Section

DQ was purified by sublimation in the dark. DMA was refluxed with acetic anhydride for 6 h and distilled under vacuum. The synthetic and purification methods of 4-chloro-*N*,*N*-dimethylaniline (4ClDMA), 4-bromo-*N*,*N*-dimethylaniline (4BrDMA), and 4-iodo-*N*,*N*-dimethylaniline (4IDMA) were described in a previous paper.[23] Fresh 1-propanol (reagent grade, Nacalai Co.) was used as the solvent without further purification.

FTEPR measurements were carried out by using an X-band pulsed EPR spectrometer (Bruker ESP 380E) equipped with a dielectric resonator (Q∼100). The methods of the electron spin−echo detection and phase correction were described elsewhere.[21,23] A microwave pulse width of 16 ns was used for the $\pi/2$ pulse. A Nd:YAG laser (Spectra-Physics GCR-150, 355 nm, 30 Hz) was utilized as the excitation light pulse. The laser power was kept low and constant at 0.5 W to avoid the hydrogen abstraction reactions that are two-photon processes. Measurements were performed with the concentration of 3×10^{-3} mol dm^{-3} for the donor and acceptor, respectively, unless

S1089-5639(98)02076-3 CCC: $15.00
Published on Web 09/26/1998

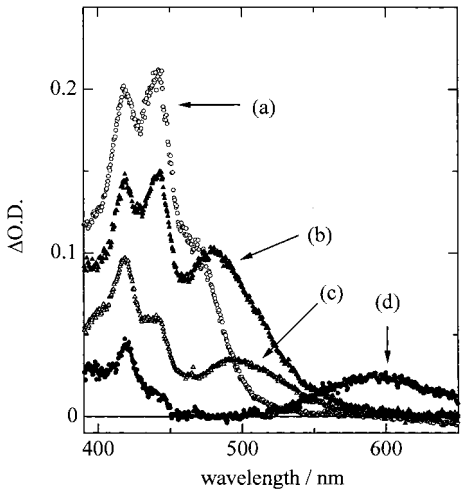

Figure 1. Transient absorption spectra obtained from the excitation of DQ in the presence of DMA (a), 4ClDMA (b), 4BrDMA (c), and 4IDMA (d) at 1 μs after the laser pulse in 1-propanol at room temperature.

otherwise stated. The sample solution was deoxygenated by argon gas bubbling and flowed into a quartz cell within the EPR resonator.

Nanosecond transient absorption spectra were measured using the multichannel analyzer controlled by a personal computer. A diode array (Princeton Instruments, IRY-700) was triggered and gated by the combined system of a digital delay/pulse generator (Stanford Research, DG-535), a pulse generator (Princeton Instruments, FG-100), and a personal computer (NEC PC-9801 BA). A Nd:YAG laser (Spectra Physik GCR-14, 355 nm, 1 Hz) was used as the light pulse source.

Results

Figure 1 shows the transient absorption spectra observed from the excitation of DQ (5×10^{-3} mol dm^{-3}) in the presence of the donor (3×10^{-3} mol dm^{-3}) of DMA (a), 4ClDMA (b), 4BrDMA (c), and 4IDMA (d) at 1 μs after the laser irradiation in 1-propanol at room temperature. The band at $\lambda_{max} = 440$ nm is attributable to the DQ anion radical, DQ$^{\bullet-}$.[27] The bands with the peaks at 465, 480, 490, and 590 nm can be assigned to the countercation radical, DMA$^{\bullet+}$, 4ClDMA$^{\bullet+}$, 4BrDMA$^{\bullet+}$ and 4IDMA$^{\bullet+}$, respectively. It should be noted that 4IDMA$^{\bullet+}$ shows a significant red shift compared with the other cation radicals of the DMA derivatives. This fact agrees well with that of the 4-iodoaniline cation radical.[28]

The present transient absorption measurements indicate that the radical yield remarkably depends on the donor. When the values of $\epsilon_{440} = 7600$ mol^{-1} cm^{-1} and $\epsilon_{490} = 5500$ mol^{-1} cm^{-1} were supposed for DQ$^{\bullet-}$ [27] and for the T−T absorption of DQ,[29] the radical yields of 0.60, 0.47, 0.21, and 0.09 were estimated for the DQ-DMA, DQ-4ClDMA, DQ-4BrDMA, and DQ-4IDMA systems, respectively. The radical yield decreased with increasing the atomic number of the heavy atoms in the donor.

Figure 2 depicts the echo-detected FTEPR spectra produced from the photolysis of DQ in the presence of DMA (a), 4ClDMA (b), 4BrDMA (c), and 4IDMA (d), respectively. The spectra were observed at the delay time of 200 ns between the laser and the first microwave pulses in 1-propanol at room temperature. The well-resolved spectra are easily assigned to DQ$^{\bullet-}$ from the EPR data of $a^H = 0.19$ mT and $g = 2.0041$. The net-emissive (E) CIDEP spectra observed in the DQ-DMA and DQ-4ClDMA systems are attributed to the TM. On the other hand, the unusual net-absorptive (A) polarization observed in the DQ-4BrDMA and DQ-4IDMA systems is ascribable to the SOCM, as reported in a previous paper.[23] No signal due to the countercation radicals was observed because of the many hyperfine splittings and short relaxation times. The very weak and complicated signals in the spectra are owing to the neutral semiquinone radical (DQH$^{\bullet}$) produced from the hydrogen abstraction. It is noteworthy that DQH$^{\bullet}$ shows net-E polarization in the DQ-4IDMA system, while DQ$^{\bullet-}$ yields net-A CIDEP. Radical pairs consisting of neutral radicals show no polarization due to SOCM in the present system.

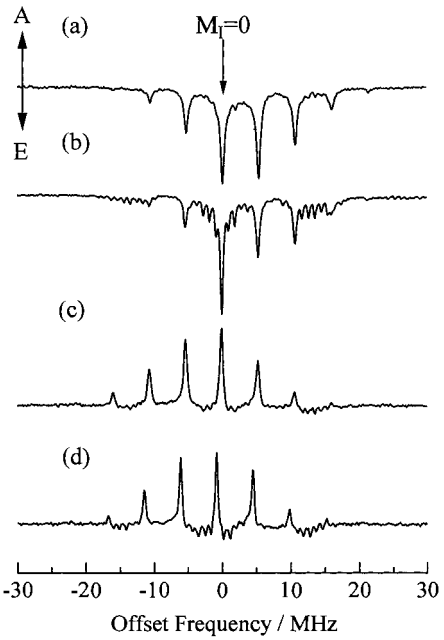

Figure 2. Echo-detected FT-EPR spectra generated from the photoexcitation of DQ in the presence of DMA (a), 4ClDMA (b), 4BrDMA (c) and 4IDMA (d) in 1-propanol at room temperature. The spectra were observed at the delay time of 200 ns between the Nd:YAG laser and the first microwave pulses. The weak and complicated signals are attributed to the duroquinone semiquinone radical produced from the hydrogen abstraction.

We are concerned with the heavy atom dependence of the net polarization. It is expected that so-called Δg-effects in the RPM also depend on the heavy atom in the donor in the present system. We determined the g values of 2.0039 and 2.0055 for 4ClDMA$^{\bullet+}$ and 4BrDMA$^{\bullet+}$, respectively, by using an in situ electrochemical method,[23] though we could not obtain the g-values for the other cation radicals. To neglect the contribution of the RPM, therefore, the hyperfine signals of $m_I = +1$, 0, -1 were plotted for DQ$^{\bullet-}$ in the DQ-DMA, DQ-4ClDMA, DQ-4BrDMA, and DQ-4IDMA systems, respectively. The time profiles obtained are shown in Figure 3, where the signal intensities are normalized with that of the thermal population. The solid lines were obtained from the nonlinear least squares curve fitting based on the kinetic equation discussed later.

In the cases of the DQ-DMA and DQ-4ClDMA systems, the net-E polarization of DQ$^{\bullet-}$ due to TM was observed. However, the maximum intensity is smaller in the DQ-4ClDMA system than in the DQ-DMA system, indicating the contribution of SOCM in the former system. In the DQ-4BrDMA system, the net-E polarization due to the TM was observed in the early time (t_d < 100 ns) and then the polarization changed to A. In contrast, only net-A CIDEP signals were measured in the DQ-4IDMA system. The buildup time constant of 60 ns is the same as that of the net-A signals in the DQ-4BrDMA system.

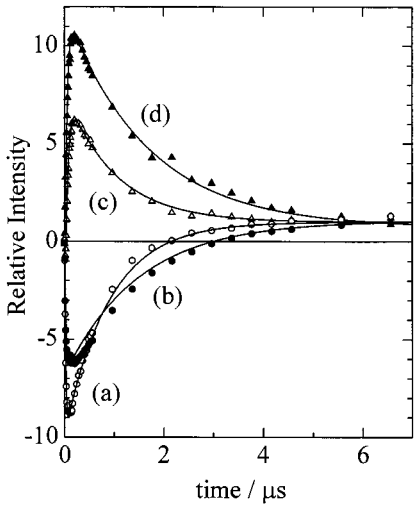

Figure 3. Time profiles of the echo-detected FT-EPR signals of the $m_I = +1$ line for DQ-DMA (a), $m_I = 0$ line for DQ-4ClDMA (b), $m_I = -1$ line for DQ-4BrDMA (c), and $m_I = -1$ line for DQ-4IDMA (d) systems, respectively, in 1-propanol at room temperature. The solid lines represent nonlinear least squares curve fits based on eq 9 and the data shown in Table 1.

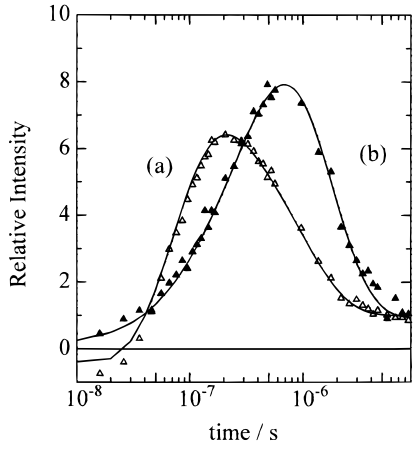

Figure 4. Donor concentration dependence of the time profiles of the hyperfine lines of $m_I = -1$ line of $DQ^{\bullet-}$ in the DQ-4BrDMA system. The measurements were carried out with the concentrations of [DQ] $= 3 \times 10^{-3}$ mol dm^{-3}, [4BrDMA] $= 3 \times 10^{-3}$ mol dm^{-3} (a), and [4BrDMA] $= 3 \times 10^{-4}$ mol dm^{-3} (b).

As shown in Figure 4, the time profiles of the FTEPR signals depend on the donor concentration. The measurements were carried out with the donor concentrations of [4BrDMA] $= 3 \times 10^{-3}$ mol dm^{-3} (a) and 3×10^{-4} mol dm^{-3} (b). Only net-A CIDEP signals were observed at the donor concentrations less than 5×10^{-4} mol dm^{-3}. The results clearly suggest that the net-A polarization is created by a bimolecular process. The solid lines are obtained from the nonlinear least squares fits based on the kinetic equation discussed later.

Discussion

Significant heavy atom effects on the radical yield and electron spin polarization were measured in the present system. The heavy atom effects can be interpreted in terms of the sublevel selective back electron transfer reaction in the ^{3}CRIP or exciplex due to SOC interaction.[23] It has been proposed that the anisotropic back electron transfer rate, $k_{ani,b}^{\mu}$ ($\mu = x, y, z$), is proportional to the amount of singlet character mixed by SOC interaction. The first-order perturbation treatment on the sandwich-type CRIP model suggests that the preferential back electron transfer occurs from the T_x and T_y sublevels to the ground state;[23]

$$k_{ani,b}^{\ z} \ll k_{ani,b}^{\ x} \sim k_{ani,b}^{\ y} \quad (1)$$

$$k_{ani,b}^{\ x} \sim k_{ani,b}^{\ y} \propto \zeta_h^{\ 2} \quad (2)$$

where the z axis is the intermolecular axis of the CRIP and ζ_h is the atomic spin−orbit coupling constant of the halogen.

In the DQ-DMA system, the radical yield of 0.6 was obtained. It might be reasonable to neglect the anisotropic back electron transfer due to heavy atom effects in this system. We supposed that a nonselective back electron transfer may be induced during the lifetime of the CRIP in this system. The isotropic back electron transfer rate is denoted as $k_{iso,b}$.

The photoinduced electron transfer in the present system occurs dominantly through the triplet process because of the very fast intersystem crossing (ISC) in DQ. This is supported by the observation of the net-E polarization in the systems of DQ-DMA, DQ-4ClDMA, and DQ-4BrDMA. We have to take into consideration several processes for the net polarization in the present system. The T_1 state of DQ gives the net-E polarization due to the TM. An electron spin polarization transfer (ESPT) from the spin-equilibrated T_1 state induces the net-A polarization.[30−33] This contribution is (4/3) times the signal intensity at the Boltzmann population in the Zeeman splitting of a radical. Heavy atom effects on the radical yield and CIDEP pattern observed in the present systems suggest that the SOC interaction contributes to the unusual net-A polarization. The concentration dependence of the buildup rate clearly indicates that this net-A polarization is generated during a bimolecular process. We can depict the electron spin polarization mechanism for the net polarization, as shown in Scheme 1.

SCHEME 1

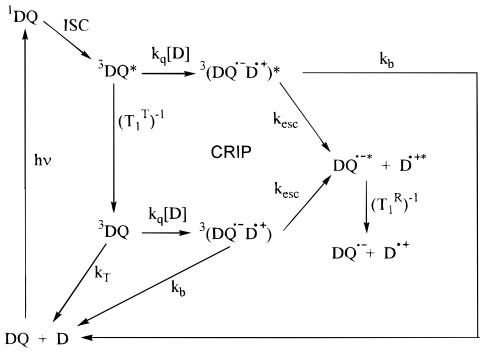

In the present analysis, the polarization due to RPM was neglected, because the time profiles shown in Figures 3 and 4 were measured for the lines with the minimum RPM contribution. The relaxation from the spin-polarized T_1 state (^{3}DQ*) to the spin-equilibrated T_1 state (^{3}DQ) competes with the quenching reaction by the electron donors (D) with the rate constant, k_q. The ^{3}CRIP or exciplex is the key intermediate in the present system, because the direct SOC interaction due to heavy atoms is short-range interaction. The initially polarized triplet CRIP, ^{3}CRIP* or ^{3}(DQ$^{\bullet-}$ D$^{\bullet+}$)*, produces the free radicals with the net-E polarization due to the TM as well as net-A created by the SOCM. In contrast, only net-A polarization should be generated in the free radicals escaping from the spin-equilibrated ^{3}CRIP, ^{3}(DQ$^{\bullet-}$ D$^{\bullet+}$), by the ESPT and SOCM.

Since ^{3}DQ is efficiently quenched by the donor in the present condition, the nonradiative path can be neglected: $k_T \ll k_q[D]$. The radical yield (ϕ_{esc}) is, therefore given by

$$\phi_{esc} = k_{esc}/(k_{esc} + k_b) \tag{3a}$$

$$k_b = k_{iso,b} + k_{ani,b} \tag{3b}$$

The k_q values are determined by the nonlinear least squares curve fitting for the buildup rate of the A-CIDEP signals due to SOCM, assuming the pseudo-first-order reaction.[23] The k_b values are obtained from the radical yield measured by the transient absorption spectra and eq 3. According to Scheme 1, we obtained a system of coupled linear first-order differential equations as follows,

$$\frac{d[^3DQ^*]}{dt} = -\frac{[^3DQ^*]}{T_1^T} - k_q[D][^3DQ^*] \tag{4}$$

$$\frac{d[^3DQ]}{dt} = \frac{[^3DQ^*]}{T_1^T} - (k_T + k_q[D])[^3DQ] \tag{5}$$

$$\frac{d[^3CRIP^*]}{dt} = k_q[D][^3DQ^*] - (k_b + k_{esc})[^3CRIP^*] \tag{6}$$

$$\frac{d[^3CRIP]}{dt} = k_q[D][^3DQ] - (k_b + k_{esc})[^3CRIP] \tag{7}$$

$$\frac{d[DQ^{\bullet-}]}{dt} = k_{esc}([^3CRIP^*] + [^3CRIP]) - k_d[DQ^{\bullet-}]^2 \tag{8}$$

The kinetic equations were solved under a steady-state approximation in the time development of the CRIP concentrations for eq 6 and 7.

Taking account that we measured the net polarization due to the SOCM and TM as well as ESPT from the thermally equilibrated ^{3}DQ, we obtained the magnetization (M_z) on the radicals based on Bloch equations,[9,34]

$$\frac{dM_z}{dt} = P_{SOCM}k_b\{[^3CRIP^*] + [^3CRIP]\}\phi_{esc} + P_{TM}k_q[D][^3DQ^*]\phi_{esc} + (4/3)P_{eq}k_q[D][^3DQ]\phi_{esc} + \frac{P_{eq}[DQ^{\bullet-}] - M_z}{T_1^R} \tag{9}$$

where the first term corresponds to the net-A polarization due to the SOCM, the second and third terms are the contribution from the TM and spin-equilibrated T_1 state and the last term represents the dynamics of the thermally populated $DQ^{\bullet-}$, respectively, in eq 9. P_{SOCM}, P_{TM}, and P_{eq} are the polarization due to SOCM, TM, and the thermal population at room temperature, respectively. We supposed that the escape rate of $k_{esc} = 1 \times 10^9$ s^{-1} in the present experimental condition.[20]

The nonlinear least squares curve fits shown in Figure 3 were performed with numerically solving the above equations by the Runge−Kutta method. A buildup time constant of 20 ns and an enhancement factor of −25 for the E-CIDEP in the DQ-DMA system were obtained from the simulation of the time profile. The rise time of the E-polarization is larger than that expected from the T_1^T value reported previously: 9.7 ns in 2-propanol.[35] A relatively slow buildup of E-TM has been reported in the photoinduced electron transfer reactions between anthraquinone and triethylamine in alcoholic solutions.[36] A detailed study would be required to determine the intrinsic enhancement factor of E-TM (V_{TM}) in the present system. The effects of the anomalous behavior in the region at the early time are considered to be negligible for the analyses of the time evolution due to SOCM, which have a relatively slow rise time. For the enhancement factor of TM (V_{TM}), McLauchlan and Sealy[37] obtained the V_{TM} values of −80 to −99 for $DQ^{\bullet-}$ generated from the photoinduced electron transfer from triethylamine in 2-propanol at 2 °C. The enhancement factor due to TM is known to depend on the reaction rate and viscosity of solvents.

TABLE 1: Fitting Parameters for CIDEP Signals of $DQ^{\bullet-}$ Generated by the Photoinduced Electron Transfer from the Donor in 1-Propanol at Room Temperature

donor	$k_q[D]/10^6$ s^{-1}	T_1^R/μs	ϕ_{esc}	$k_{ani,b}/k_{esc}$	V_{SOCM}
DMA	25	1.2	0.60	0	0
4ClDMA	25	1.5	0.47	0.46	2(±2)
4BrDMA	20	1.3	0.21	3.1	17(±1)
4IDMA	20	1.6	0.09	9.4	25(±1)

On the basis of these data, we analyzed the time evolution of the CIDEP signals observed in the other systems. Since the buildup time constant of the E polarization, the rise time of the A-CIDEP signals, and the decay of the CIDEP signals are different from each other, we can perform the curve fitting easily. We obtained the intrinsic enhancement factors due to the SOCM of $V_{SOCM} = P_{SOCM}/P_{eq} = 17$ and 25 for the DQ-4BrDMA and DQ-4IDMA systems, respectively. For the DQ-4ClDMA, a V_{SOCM} value of about 2 reproduced the time evolution of the signal, but there exist some residuals in the fits. The small *g*-effect seems to induce some uncertainty because of the minor effect of the SOCM in this system. The enhancement factors and kinetic parameters determined are summarized in Table 1.

From the curve fitting shown in Figure 3, we obtained the decay time constant of 1.2−1.6 μs. We tentatively regard the time constant as T_1^R, though these values are much smaller than those reported previously: $T_1^R = 6.7$ μs in 2-propanol at 20 °C.[38,39] The variation of the time constants was negligible at concentrations less than 5×10^{-3} mol dm^{-3}. Thus, the electron transfer reaction between $DQ^{\bullet-}$ and DQ is unimportant at the present condition. The T_1^R of $DQ^{\bullet-}$ is likely to be reduced by long-range interaction between the acceptor and donor ion radicals in the present systems.

As shown in Figure 4, the time profiles observed in the different concentrations of 4BrDMA are also well reproduced by using the same data set. In the DQ-4ClDMA and DQ-4IDMA systems, the consistent results were obtained for the donor concentration dependence of the time profiles.

Figure 5 shows the plots of the $k_{ani,b}/k_{esc}$ vs the square of the SOC constant of halogen in the donor. The good linear relationship obtained indicates the validity of the present treatment.

The $V_{SOCM}(Cl)/V_{SOCM}(Br)$ value agrees well with the square of ζ_{Cl}/ζ_{Br}. In contrast, the intrinsic enhancement factor in the DQ-4IDMA system is not much different from that in the DQ-4BrDMA system. This is considered to be due to the lowering of the sublevel selectivity in the back electron transfer. The relative radical yield in the DQ-4IDMA system, $\phi_{esc}^r = \phi_R(I)/\phi_R(H) = 0.15$ is smaller than that of the ideal sublevel selective back electron transfer (0.33), indicating that the iodine atom

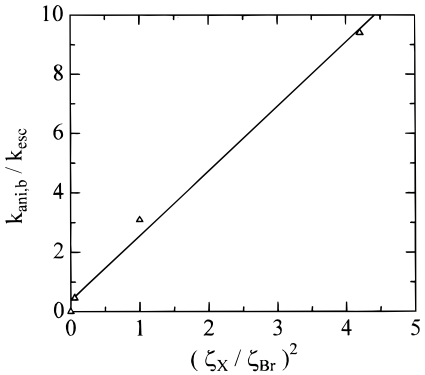

Figure 5. Plots of $k_{ani,b}/k_{esc}$ vs the square of the SOC constant of halogen in the donor.

enhances isotropic back electron transfer as well the sublevel selective one.

In the slow rotational limit, the theoretical enhancement factor is described as follows,[23]

$$V_{SOCM} = \frac{8DK}{15\omega_0}\frac{2kT}{g\beta B_0} \tag{10}$$

where $K = \{(k_{ani,b}{}^x + k_{ani,b}{}^y)/2 - k_{ani,b}{}^z\}/(k_{ani,b}{}^x + k_{ani,b}{}^y + k_{ani,b}{}^z)$ and the ideal sublevel back electron transfer yields a K value of 0.5. The other notations have their usual meaning. Thus, the D value of 0.02 cm^{-1} is estimated for ^{3}CRIP in the DQ-4BrDMA system from eq 10. On the other hand, the D value is considered to be larger than 0.03 cm^{-1} in the DQ-4IDMA system, because the K value would be smaller than that of the ideal case. As discussed above, the isotropic back electron transfer is enhanced in this system.

Since the SOC interaction is the short-range interaction, a sandwich-type geometry may be postulated for ^{3}CRIP.[19,23] From the net-A polarization observed in the SOCM, sublevel selective back electron transfer occurs preferentially from the upper sublevel(s). The SOC interaction due to heavy atoms induces the preferential back electron transfer from the T_x and T_y sublevels; $k_{ani,b}{}^x \; k_{ani,b}{}^y \gg k_{ani,b}{}^z$, where the z axis is the intermolecular axis of the sandwich-type CRIP. Therefore, the spin polarization observed clearly suggests that the T_x and T_y sublevels are higher than the T_z state in energy; $D > 0$. A simple treatment by the electron spin dipolar interaction cannot explain such a positive D value in ^{3}CRIP.

Taking into account the solvent coordinate, the level crossing between the potential surfaces of the ^{1}CRIP and ground states induces the mixing between these states.[40] The mixed state is lower than the ^{3}CRIP state in energy, because they cross in the Marcus normal region: the charge recombination energy $\Delta G_{CR} = E_{1/2}{}^{red}(DQ) - E_{1/2}{}^{ox}(DMA) = -1.54$ eV. When the ^{3}CRIP state interacts with the lower lying mixed singlet state through the SOC interaction, the positive D value is obtained as shown in Figure 6. It can be deduced that the D value increases with increasing atomic number of heavy atoms. The preferential mixing of the singlet charge transfer state in the T_x and T_y sublevels may induce efficient sublevel selective back electron transfer, leading to a net-A-polarization.

Conclusion

Heavy atom effects on the radical yield and CIDEP spectra were quantitatively studied for the photoinduced electron transfer reactions between DQ and DMA as well as its monohalogen substituents. The radical yield decreases with increasing the atomic number of the halogen substituents in the electron donor which are not directly excited. We analyzed the influence of heavy atoms and the donor concentration on the time evolution of the electron spin polarization. The net polarization was interpreted in terms of the contribution of the E-TM, the net-A polarization due to the SOCM, and the ESPT from the thermally equilibrated triplet precursor. The intrinsic enhancement factors due to SOCM were determined to be $V_{SOCM} = P_{SOCM}/P_{eq} = 2$, 17, and 25 for the DQ-4ClDMA, DQ-4BrDMA, and DQ-4IDMA systems, respectively. The net-A polarization observed suggests a positive D value for ^{3}CRIP of the DQ-4XDMA systems, indicating that the SOC interaction with the ground-state governs the ZFS parameters.

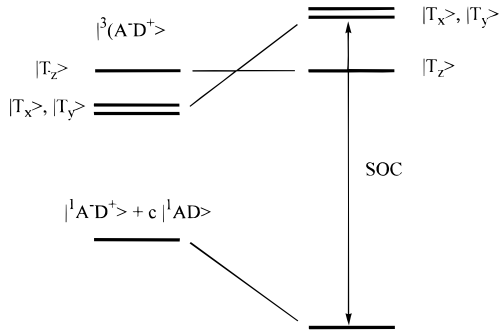

Figure 6. Schematic energy diagram for the triplet sublevels of CRIP.

Acknowledgment. The present research was supported in part by a Grant-in-Aid of Scientific research (No. 07404040) from the Ministry of Education, Science, Sports, and Culture, Japan.

References and Notes

(1) Adrian, F. J. *J. Chem. Phys*. **1971**, *54*, 3912, 3918.
(2) Pedersen, J. B.; Freed, J. H. *J. Chem. Phys*. **1973**, *58*, 2746.
(3) Wong, S. K.; Hutchison, D. A.; Wan, J. K. S. *J. Chem. Phys*. **1973**, *58*, 985.
(4) Atkins, P. W.; Evans, G. T. *Mol. Phys*. **1974**, *27*, 1633.
(5) Pedersen, J. B.; Freed, J. H. *J. Chem. Phys*. **1975**, *62*, 1706.
(6) Buckley, C. D.; McLauchlan, K. A. *Chem. Phys. Lett*. **1987**, *137*, 86.
(7) Closs, G. L.; Forbes, M. D. E.; Norris, J. R. *J. Phys. Chem*. **1987**, *91*, 3592.
(8) Blätter, C.; Jent, F.; Paul, H. *Chem. Phys. Lett*. **1990**, *166*, 375.
(9) Blätter, C.; Paul, H. *Res. Chem. Intermed.* **1991**, *16*, 201.
(10) Goudsmit, G.-H.; Paul, H.; Shushin, A. I. *J. Phys. Chem.* **1993**, *97*, 13243.
(11) Kawai, A.; Okutsu, T.; Obi, K. *J. Phys. Chem.* **1991**, *95*, 9130.
(12) Kawai, A.; Obi, K. *J. Phys. Chem.* **1992**, *96*, 52, 5701.
(13) Kobori, Y.; Kawai, A.; Obi, K. *J. Phys. Chem.* **1994**, *98*, 6425.
(14) Jenks, W. S.; Turro, N. J. *J. Am. Chem. Soc*. **1990**, *112*, 9009.
(15) Turro, N. J.; Khudyakov, I. V.; Bossmann, S. H.; Dwyer, D. W. *J. Phys. Chem.* **1993**, *97*, 1138.
(16) Step, E. N.; Buchachenko, A. L.; Turro, N. J. *J. Am. Chem. Soc.* **1994**, *116*, 5462.
(17) Steiner, U. E. *Ber. Bunsen-Ges. Phys. Chem*. **1981**, *85*, 228.
(18) Ulrich, T.; Steiner, U. E.; Föll, R. E. *J. Phys. Chem.* **1983**, *87*, 1873.
(19) Steiner, U. E.; Ulrich, T. *Chem. Rev.* **1989**, *89*, 51.
(20) Steiner, U. E.; Haas, W. *J. Phys. Chem.* **1991**, *95*, 1880.
(21) Katsuki, A.; Akiyama, K.; Ikegami, Y.; Tero-Kubota, S. *J. Am. Chem. Soc*. **1994**, *116*, 12065.
(22) Katsuki, A.; Akiyama, K.; Tero-Kubota, S. *Bull. Chem. Soc. Jpn*. **1995**, *68*, 3383.
(23) Sasaki, S.; Katsuki, A.; Akiyama, K.; Tero-Kubota, S. *J. Am. Chem. Soc*. **1997**, *119*, 1323.
(24) Kleverlaan, C. J.; Martino, D. M.; van Willigen, H.; Stufkens, D. J.; Oskam, A. *J. Phys. Chem.* **1996**, *100*, 18607.
(25) Leung, M.; El-Sayed, M. A. *J. Am. Chem. Soc*., **1975**, *97*, 669.
(26) Dellinger, B.; Hochstrasser, R. M.; Smith, A. B. *J. Am. Chem. Soc*. **1977**, *99*, 5834.
(27) Patel, K. B.; Willson, R. L. *J. Chem. Soc., Faraday Trans. 1* **1973**, *69*, 814.

(28) Jonsson, M.; Lind, J.; Eriksen, T. E.; Merenyi, G. *J. Am. Chem. Soc*. **1994**, *116*, 1423.
(29) Amouyal, E.; Bensasson, R. *J. Chem. Soc., Faraday Trans. 1* **1976**, *72*, 1274.
(30) Paul, H. *Chem. Phys*. **1979**, *40*, 265; **1979**, *43*, 294.
(31) Levstein, P. R.; van Willigen, H. *J. Chem. Phys*. **1991,** *95*, 900.
(32) van Willigen, H.; Levstein, P. R.; Ebersole, M. H. *Chem. Rev*. **1993**, *93*, 173.
(33) Akiyama, K.; Sekiguchi, S.; Tero-Kubota, S. *J. Phys. Chem*. **1996**, *100*, 180.
(34) Pedersen, J. B. *J. Chem. Phys*. **1973**, *59*, 2656.
(35) Atkins, P. W.; Dobbs, A. J.; McLauchlan, K. A. *Chem. Phys. Lett*. **1974**, 29, 616.
(36) Beckert, D.; Plüschau, M.; Dinse, K. P. *J. Phys. Chem*. **1992**, 96, 3193.
(37) McLauchlan, K. A.; Sealy, G. R. *Mol. Phys*. **1984**, 52, 783.
(38) Hore, P. J.; McLauchlan, K. A. *Chem.* Phys. *Lett*. **1980**, 75, 582.
(39) Hore, P. J.; McLauchlan, K. A. *Mol. Phys*. **1981**, 42, 1009.
(40) Sekiguchi, S.; Kobori, Y.; Akiyama, K.; Tero-Kubota, S. *J. Am. Chem. Soc*. **1998**, *120*, 1325.